Available online at www.sciencedirect.com
SCIENCE DIRECT®
International Journal of Heat and Mass Transfer 47 (2004) 5181–5188
International Journal of HEAT and MASS TRANSFER
www.elsevier.com/locate/ijhmt

# Experimental investigation into convective heat transfer of nanofluids at the entrance region under laminar flow conditions

Dongsheng Wen, Yulong Ding *

*Institute of Particle Science and Engineering, University of Leeds, Leeds LS2 9JT, UK*

Received 24 March 2004; received in revised form 13 July 2004

**Abstract**

This paper reports an experimental work on the convective heat transfer of nanofluids, made of $\gamma$-$Al_2O_3$ nanoparticles and de-ionized water, flowing through a copper tube in the laminar flow regime. The results showed considerable enhancement of convective heat transfer using the nanofluids. The enhancement was particularly significant in the entrance region, and was much higher than that solely due to the enhancement on thermal conduction. It was also shown that the classical Shah equation failed to predict the heat transfer behaviour of nanofluids. Possible reasons for the enhancement were discussed. Migration of nanoparticles, and the resulting disturbance of the boundary layer were proposed to be the main reasons.


*Keywords:* Nanofluids; Convective heat transfer; Laminar flow; Entrance region; Nanoparticles

## 1. Introduction

Heat transfer fluids such as water, minerals oil and ethylene glycol play an important role in many industrial sectors including power generation, chemical production, air-conditioning, transportation and microelectronics. The performance of these conventional heat transfer fluids is often limited by their low thermal conductivities. Driven by industrial needs of process intensification and device miniaturization, development of high performance heat transfer fluids has been a subject of numerous investigations in the past few decades. As solids materials in particular metals can have very high thermal conductivities, lots of studies have been carried out in the past on the thermal behaviour of suspensions of particulate solids in liquids; see for example [1–4]. These early studies, however, used suspensions of millimeter or micrometer sized particles, which, although showed some enhancement, experienced problems such as poor suspension stability and hence channel clogging, which are particularly serious for systems using mini- and/or micro-channels.

Recent advances in nanotechnology have allowed development of a new category of fluids termed nanofluids. Such fluids are liquid suspensions containing particles that are significantly smaller than 100 nm, and have a bulk solids thermal conductivity of orders of

* Corresponding author. Tel.: +44 113 343 2747; fax: +44 113 243 2405.
*E-mail address:* y.ding@leeds.ac.uk (Y. Ding).

0017-9310/$ - see front matter © 2004 Elsevier Ltd. All rights reserved.
doi:10.1016/j.ijheatmasstransfer.2004.07.012

**Nomenclature**

| | |
|---|---|
| $A$ | tube cross-sectional area |
| $D$ | tube diameter |
| $c_p$ | fluid heat capacity |
| $d_p$ | particle diameter |
| $h$ | heat transfer coefficient |
| $k$ | fluid thermal conductivity |
| $Nu$ | Nusselt number |
| $Pe$ | Peclet number, $Pe = \dot{\gamma} \cdot d_p^2/v$ |
| $Pr$ | Prandtle number |
| $q$ | Heat flux |
| $Re$ | Reynolds number, $Re = \rho u D/\mu$ |
| $S$ | perimeter of tube |
| $T$ | temperature |
| $u$ | fluid velocity |
| $x$ | axial distance |

*Greek symbols*

| | |
|---|---|
| $\alpha$ | fluid thermal diffusivity |
| $\delta_t$ | thermal boundary layer thickness |
| $\Phi$ | volume fraction |
| $\dot{\gamma}$ | fluid shear rate |
| $v$ | fluid kinematic viscosity |
| $\mu$ | fluid viscosity |
| $\rho$ | fluid density |

*Subscripts*

| | |
|---|---|
| f | fluid |
| in | inlet |
| L | base liquid |
| w | wall |

magnitudes higher than the base liquids. The term of nanofluids was first used by the group at the Argonne National Laboratory, USA, about a decade ago [5], but equal credit should also be given to some earlier workers such as Masuda et al. [6]. The potential advantages of properly engineered nanofluids include (a) higher thermal conductivities than that predicted by currently available macroscopic models, (b) excellent stability, and (c) little penalty due to an increase in pressure drop and pipe wall abrasion experienced by suspensions of millimeter or micrometer particles. As a consequence, a number of experimental studies have been performed to investigate the transport properties of nanofluids in the past decade; see for examples [5–14]. Most of these studies are on the effective thermal conductivity under macroscopically stationery conditions. There are very few studies on other aspects related to nanofluids such as phase change behaviour [15–20] and convective heat transfer [21–26]. Even of these few studies, there are some controversial results. For example, Pak and Cho [22] investigated convective heat transfer in the turbulent flow regime using water–$Al_2O_3$ and water–$TiO_2$ nanofluids, and found that the Nusselt number of the nanofluids increased with increasing volume fraction of the suspended nanoparticles, and the Reynolds number. However, for a given average fluid velocity, the convective heat transfer coefficient of a nanofluid with 3 vol.% nanoparticles was 12% lower than that of pure water. This appears to disagree with the observation of Lee and Choi [21] and Xuan and Li [25]. Lee and Choi [21] studied convective heat transfer of laminar flows of an unspecified nanofluid in microchannels, and observed a reduction in thermal resistance by a factor of 2. Nanofluids were also observed to be able to dissipate a heat power three times more than pure water could do. Xuan and Li [25] measured convective heat transfer coefficient of water–Cu nanofluids, and found substantial heat transfer enhancement. For a given Reynolds number, heat transfer coefficient of nanofluids contained ~2 vol.% Cu nanoparticles was shown to be approximately 60% higher than that of pure water.

This work aims at more fundamental understanding of the convective heat transfer behaviour of nanofluids. The focus will be on the entrance region under the laminar flow conditions, for which no previous studies have been found in the literature. Aqueous based nanofluids containing $\gamma$-$Al_2O_3$ nanoparticles of various concentrations will be tested under the constant heat flux boundary condition. The results will be compared with conventional theories, and the mechanisms for the enhancement of convective heat transfer will be discussed.

## 2. Experimental

### 2.1. Experimental system

The experimental system constructed for this work is shown schematically in Fig. 1. It consisted of a flow loop, a heating unit, a cooling part, and a measuring and control unit. The flow loop included a pump with a built-in flowmeter, a reservoir, a collection tank and a test section. A straight copper tube with 970 mm length, $4.5 \pm 0.02$ mm inner diameter, and $6.4 \pm 0.05$ mm outer diameter was used as the test section. The whole test section was heated by a silicon rubber flexible heater (Watlow, UK) linked to a DC power supply (TTi Ex 752m, RS, UK). The power supply was adjustable and had a maximum power of 300 W. There

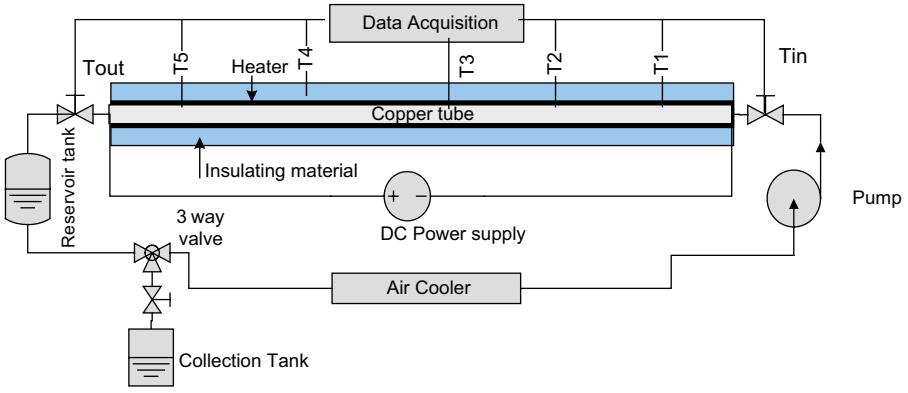


Fig. 1. Experimental system.

was a thick thermal isolating layer surrounding the heater to obtain a constant heat flux condition along the test section; see Section 2.3 for more details. Five T-type thermocouples were mounted on the test section at axial positions in mm of 118 (T1), 285 (T2), 524 (T3), 662 (T4) and 782 (T5) from the inlet of the test section to measure the wall temperature distribution, and two further T-type thermocouples were inserted into the flow at the inlet and exit of the test section to measure the bulk temperatures of nanofluids. The pump used in this work was of peristaltic type with flowrate controlled by the rotational rate. The maximum flow rate the pump could deliver was 10 l/min. There was a three-way valve in the flow loop for flowrate calibrations and flow system cleaning between runs even with the same nanofluid.

### 2.2. Calibration of experimental devices

In the heat transfer experiments, the pump rotational rate, voltage and current of the DC power supply were recorded and the temperature readings from the seven thermocouples were registered by a data requisition system. As the pump performance was sensitive to the fluid viscosity at a given rotational speed, calibration was needed, which was carried out before and after each experiment by a weighing method. This gave an accuracy of nanofluids flowrate better than 4.6%. The thermocouples were calibrated in a thermostat water bath and the accuracy was found to be within 0.1 K.

### 2.3. Data processing

The heat transfer performance of flowing nanofluids was defined in terms of the following convective heat transfer coefficient ($h$) and the Nusselt number ($Nu$):

$$h(x) = q/(T_w(x) - T_f(x)) \tag{1}$$

$$Nu(x) = h(x)D/k \tag{2}$$

where $q$ is the heat flux, $T_w$ and $T_f$ are, respectively, the wall and fluid temperatures, $D$ is the tube diameter, $k$ is the fluid thermal conductivity, and $x$ represents axial distance from the entrance of the test section. The fluid temperature profile in the test section was obtained through the energy balance:

$$T_f(x) = T_{in} + qSx/(\rho c_p uA) \tag{3}$$

where $c_p$ is the heat capacity, $\rho$ is the fluid density, $A$ and $S$ are, respectively, the cross-sectional area and perimeter of the test tube, and $u$ is the average fluid velocity. Eq. (3) is based on an assumption of zero heat loss through the insulation layer. The deviation to this assumption was assessed by comparing the measured temperature difference between inlet and outlet of the test section with the theoretical value calculated by Eq. (3). It was found that the deviation was lower than 6.2% under the conditions of this work.

Traditionally, the Nusselt number is related to the Reynolds number defined as $Re = \rho uD/\mu$ and the Prandtle number defined as $Pr = \nu/\alpha$, where $\nu$ is the fluid kinematic viscosity, $\alpha$ is the fluid thermal diffusivity, and $\mu$ the fluid dynamic viscosity. This requires the knowledge of the transport properties of nanofluids, in particular viscosity and thermal conductivity. As very dilute suspensions were used in this work (see later for details), the Einstein equation was used to estimate the viscosity of nanofluids:

$$\mu = \mu_L(1 + 2.5\Phi) \tag{4}$$

where $\mu_L$ is the viscosity of the base liquid, and $\Phi$ is the volume fraction of nanoparticles. Eq. (4) applies to suspensions of low particle concentrations (usually <2 vol.%), where particle-particle interactions are negligible. The thermal conductivity of nanofluids was determined by experiments; see later for details.

It should be noted that the transport properties are functions of temperature. As a consequence, the viscosity was calculated by using the mean fluid temperature

between the inlet and outlet, while the thermal conductivity was measured at different temperatures.

### 2.4. Preparation of nanofluids

Nanoparticles used in this work were $\gamma$-$Al_2O_3$ with a size range of 27–56 nm, supplied by Nanophase Technologies, US. De-ionized water was used as the base liquid. A small amount (one tenth of the mass of nanoparticles) of sodium dodecylbenzene sulfonate (SDBS, Aldrich-Sigma Corp.) was used as the dispersant to stabilize the nanoparticles. The dispersant was first mixed with water. Nanoparticles were then dispersed into water and the mixture was sonicated continuously for 16–20 h in an ultrasonic bath (Grant MXB6, UK). Nanofluids with less than 4 wt.% nanoparticles were found very stable and the stability lasted over a week; some sedimentation was found for mass concentrations more than 4 wt.% after 4 h, however it was still long enough for the experiments. Fig. 2 shows an SEM image of a nanofluid with 1.0% volume concentration of $Al_2O_3$. The effective thermal conductivity of nanofluids was measured by using a KD2 thermal property meter (Labcell Ltd, UK), which is based on the transient hot wire method. The uncertainty of the measurements was within 3% under the conditions of this work. A typical set of results is shown in Fig. 3 for measurements at 22 °C, where $k_L$ is the thermal conductivity of the base liquid (water). Also shown in the figure are predictions by the Maxwell–Garnett (MG) [27], the Bruggeman [27], the differential effective medium theory (DEMT) [28], and the Hamilton and Crosser (HC) [29] models developed for macroscopic systems. It can be seen that the effective thermal conductivity of nanofluids increases approximately linearly with particle volume fraction, and the macroscopic models fail to predict the measured results.

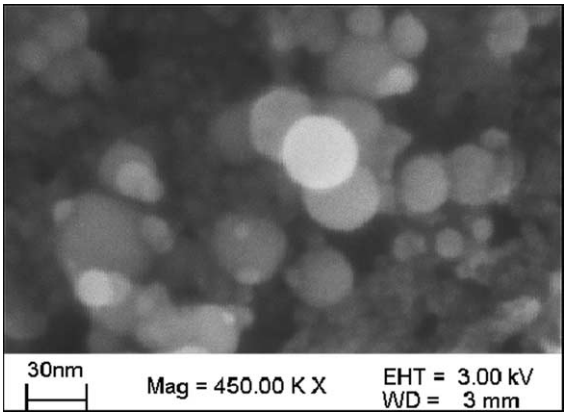


Fig. 2. SEM image of 1 vol.% dispersed $Al_2O_3$ nanoparticle in water.

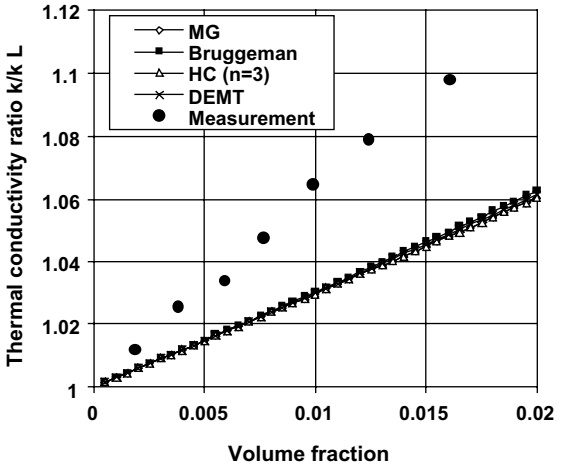


Fig. 3. Effective thermal conductivity of $Al_2O_3/H_2O$ nanofluids at 22 °C.

### 2.5. Initial tests of the experimental system against water

Before conducting systematic experiments on nanofluids, the reliability and accuracy of the experimental system were tested using de-ionized water as the working fluid. The results were compared with the predictions of the following well-known Shah equation for laminar flows under the constant heat flux boundary condition [30]:

$$Nu = \begin{cases} 1.953\left(RePr\frac{D}{x}\right)^{1/3} & \left(RePr\frac{D}{x}\right) \geqslant 33.3 \\ 4.364 + 0.0722RePr\frac{D}{x} & \left(RePr\frac{D}{x}\right) < 33.3 \end{cases} \quad (5)$$

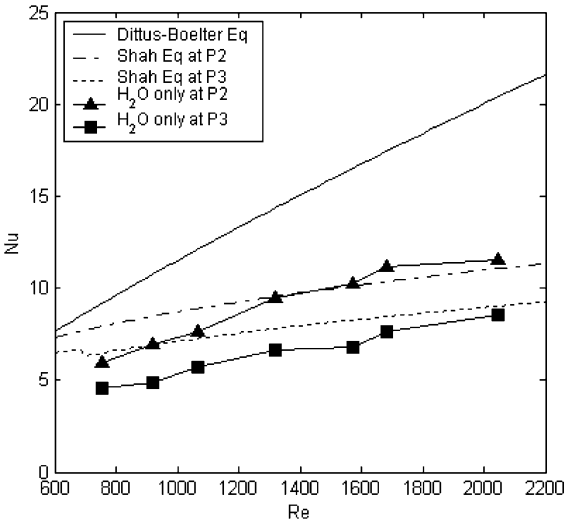


Fig. 4. Comparisons with Shah equation at P2 and P3, water flow.

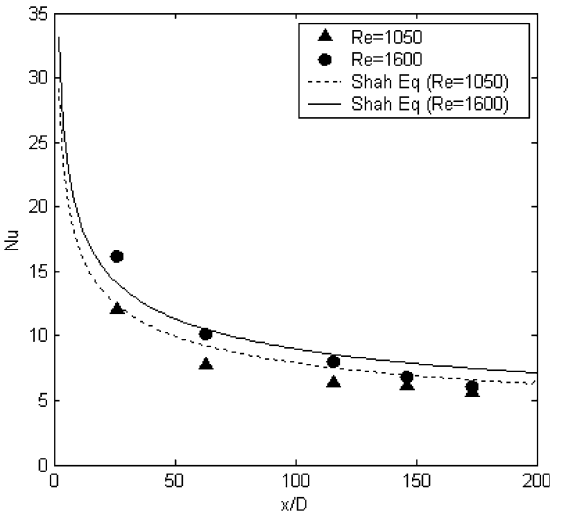


Fig. 5. Comparisons with Shah equation along axial direction, water flow.

Fig. 4 shows a comparison between the classical Shah equation and the measurements using de-ionized water at Position 2 ($x = 285$ mm) and 3($x = 524$ mm) corresponding to the thermocouples $T_2$ and $T_3$ in Fig. 1. For reference, predictions by the following Dittus–Boelter (D–B) equation for turbulent flows are also included:

$$Nu = 0.023Re^{0.8}Pr^{0.4} \quad (6)$$

Reasonably good agreement can be seen between the Shah equation and the measurements over the Reynolds number range used in this work. The discrepancy occurs mainly at low Reynolds number range, e.g. the measured value is about 24% lower at P2, and 30% lower at P3 than the corresponding predictions at the lowest Reynolds number tested. The discrepancy decreases to within 5% at the Reynolds number over about 2000. The axial profile of local Nusselt number is shown in Fig. 5 at Reynolds numbers of 1050 and 1600. Again, reasonably good agreement is seen and the maximum discrepancy is ~18% at Position 5 ($x = 782$ mm) for the Reynolds number of 1600. The exact reason for the discrepancy is unclear; difference in the tube size may be one of the reasons. The Shah equation was developed on the basis of laminar flows in large channels, whereas a relatively small tube was used in this work; see for example [31,32].

## 3. Experimental results

Having built-up confidence in the experimental system, systematic experiments were performed over a Reynolds number of 500–2100. The results are presented and discussed in this section.

### 3.1. Axial profiles of the convective heat transfer coefficient

Figs. 6 and 7 plot the local heat transfer coefficient against the axial distance from the entrance of the test section at two Reynolds numbers (Due to small variation in viscosity at different particle concentrations, refer to Eq. (4), the Reynolds number changes slightly even at a given fluid velocity. The changes in the values of Reynolds number in Figs. 6 and 7 are within ±50). The results clearly show that the use of nanofluids significantly improves the convective heat transfer, in particularly at the entrance region and at the higher Reynolds number. For nanofluids containing 1.6% nanoparticles by volume, the local heat transfer coefficient at Position 2

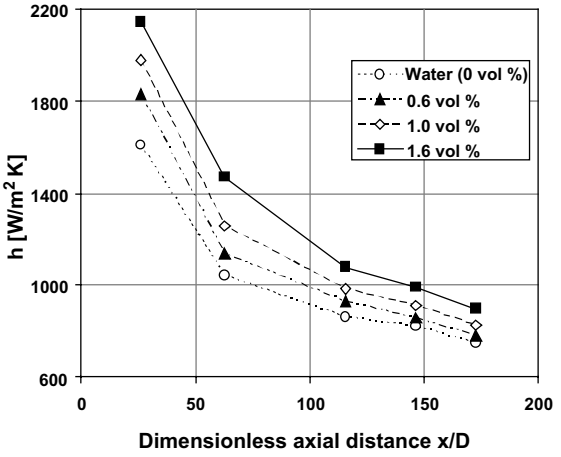


Fig. 6. Axial profile of local heat transfer coefficient ($Re = 1050 \pm 50$).

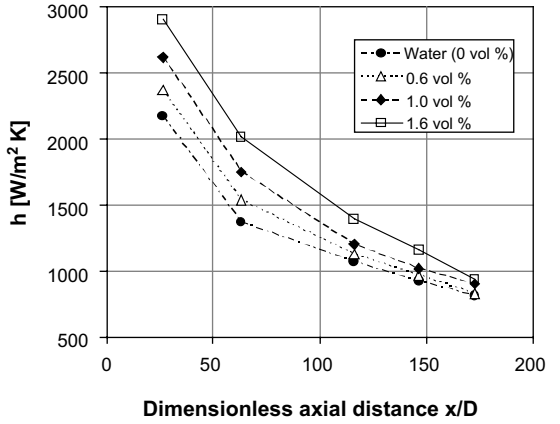


Fig. 7. Axial profile of local heat transfer coefficient ($Re = 1600 \pm 50$).

($x = 285$ mm, $x/D \sim 63$) is, respectively, ~41% and ~47% higher at $Re = 1050$ and 1600 in comparison with the case of water only. The local heat transfer coefficient is also seen to increase with particle concentration. Figs. 6 and 7 also show a significant decrease in the heat transfer enhancement with increasing distance from the entrance region. For the nanofluid with 1.6% by volume nanoparticles, the enhancement decreases from ~47% at Position 2 ($x/D \sim 63$) to ~14% at Position 5 ($x/D \sim 173$) at $Re = 1600$. This behaviour indicates that 'smart' measures could be taken when using nanofluids for heat transfer enhancement. For example, one may create 'artificial entrance' regions along a pipeline to maximize the performance of nanofluids. An inspection of Figs. 6 and 7 also indicates that the thermal entrance length of nanofluid flows is longer than that of pure base liquid flows.

A comparison of the results in Figs. 6 and 7 with those in Fig. 3 shows that the enhancement of the local heat transfer coefficient is much more dramatic than the enhancement of the effective thermal conductivity in most part of the test section. A similar trend was also observed by Xuan and Li [25] in the turbulent flow regime. They showed that the local heat transfer coefficient increased to ~60% for a water based nanofluid containing 2% Cu nanopaticles by volume, and the nanofluids only had an effective thermal conductivity approximately 12.5% higher than that of the base liquid. A number of reasons may be responsible for the enhancement; see Section 3.3 for a more detailed discussion.

### 3.2. Dependence of the Nusselt number on the Reynolds number

The relationships between Nusselt number and Reynolds number at Positions 2 and 3 are shown, respectively, in Figs. 8 and 9. Predictions by the classical Shah equation for laminar flows and Dittus–Boelter equation for turbulent flows are also included for comparison. It can be seen that the measured Nusselt number for nanofluids is higher than that for water, and the Shah equation fails to predict the measured results. The enhancement is also seen to increase with Reynolds number and nanoparticle volume concentration, and is more significant at the entrance region of the test section.

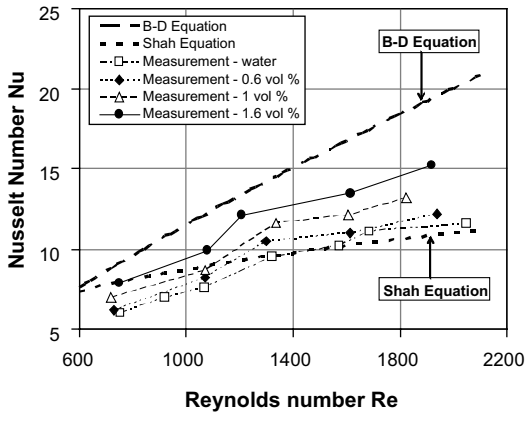


Fig. 8. Dependence of Nusselt number on Reynolds number at Position 2 ($x/D = 63$).

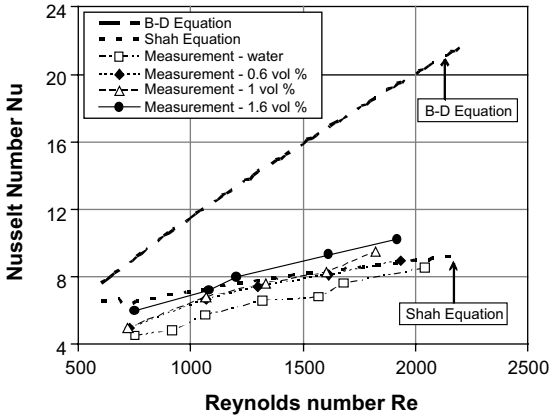


Fig. 9. Dependence of Nusselt number on Reynolds number at Position 3 ($x/D = 116$).

### 3.3. Discussion on the mechanisms for the enhancement

Before discussing possible enhancement mechanisms, it is helpful to have a look at some earlier studies on heat transfer of slurry flows with micrometer or millimeter particles, which have shown that the addition of particles could enhance heat transfer coefficient [1–3]. Sohn and Chen [1] measured the effective thermal conductivity in a rotating Couette flow apparatus at low Reynolds number but high Peclet number conditions, where the Peclet number is defined as $\dot{\gamma} \cdot d_p^2/v$ with $\gamma$ the shear rate, and $d_p$ particle diameter. Significant enhancement on effective thermal conductivity was observed at the Peclet number over 300, and the shear-dependent behaviour fitted well into a power law relationship at $Pe > 300$. A similar trend was also reported by Ahuja [2]. He used a shell-and-tube heat exchanging arrangement, and employed the Graetz solutions at the entrance region to evaluate the effective thermal conductivity of a saline/polystyrene latex suspension. These researchers attributed the enhancement to the high Peclet number, which represents a measure of the eddy scale convection as compared to conduction, and therefore is associated with self-rotating and/or microconvection [2,3]. In nanofluids heat transfer, the length scale of nanoparticles and hence the Peclet number is of an order of 1. As a conse-

quence, the enhancement on the local heat transfer coefficient of nanofluids cannot be interpreted using the same argument proposed for the micron or millimeter sized particle suspensions.

The local heat transfer coefficient, $h$, can be approximately given as $k/\delta_t$ with $\delta_t$ the thickness of thermal boundary layer. This indicates that two parameters, $k$ and $\delta_t$, affect the convective heat transfer coefficient. Both an increase in $k$ and/or a decrease in $\delta_t$ increase the convective heat transfer coefficient. The effective thermal conductivity of nanofluids has been studied by a number of investigators as briefly summarized in the introduction section, and a number of mechanisms have been proposed for the enhancement including the interfacial layering, Brownian motion, ballistic transport of energy carriers, and clustering, etc.; see for example [12]. As seen from Fig. 3, the maximum enhancement on the thermal conductivity is ~10% under the conditions of this work, whereas the enhancement on the convective heat transfer is much higher in the entrance regime, and gradually approaches a constant (Figs. 6 and 7). The big enhancement in the entrance region can therefore be attributed to a decrease in the thermal boundary layer thickness. The exact mechanisms for the reduction in the thermal boundary are unclear. One of the possible reasons is particle migration in nanofluids due to shear action, viscosity gradient, and Brownian motion in the cross-section of the tube; see for example [33]. Wen and Ding [34] investigated particle migration in nanofluids flowing through a tube and its effect on heat transfer by using a theoretical model. They found that particle migration due to these effects could result in a significant non-uniformity in particle concentration across the tube cross-section, in particular for relatively large particles. Particle migration is expected to be more significant in the entrance region due to larger velocity gradient. The non-uniform particle concentration also has a significant influence on the local thermal conductivity and viscosity. Compared with the constant thermal conductivity assumption, the non-uniform thermal conductivity profile resulting from particle migration showed a higher Nusselt number, and the extent of the Nusselt number increase depended on the Peclet number and mean particle concentration.

The presence of nanoparticles also affects the boundary layer development in pipe flows and hence heat transfer. For pure liquids, the boundary layer develops smoothly and flows are hydrodynamically fully developed after $x \sim (0.05Re)\cdot D$, whereas they are thermally fully developed after $x \sim (0.05RePr)\cdot D$. Figs. 6 and 7 clearly show existence of a greater thermal developing length for nanofluids, which increases with increasing particle concentrations. The effect of particles on the boundary layer development has also been suggested to be the main mechanism for heat transfer enhancement in particulate flow under turbulent regime [4].

## 4. Conclusions

This paper is concerned with the convective heat transfer of nanofluids made of water and $\gamma$-$Al_2O_3$ nanoparticles. Experiments were carried out in the laminar flow regime. The following conclusions were obtained:

- The use of $Al_2O_3$ nanoparticles as the dispersed phase in water can significantly enhance the convective heat transfer in the laminar flow regime, and the enhancement increases with Reynolds number, as well as particle concentration under the conditions of this work.
- The enhancement is particularly significant in the entrance region, and decreases with axial distance. The thermal developing length of nanofluids is greater than that of pure base liquid, and is increasing with an increase in particle concentration.
- The enhancement of the convective heat transfer could not be solely attributed to the enhancement of the effective thermal conductivity. Particle migration is proposed to be a reason for the enhancement, which results a non-uniform distribution of thermal conductivity and viscosity field and reduces the thermal boundary layer thickness.

## Acknowledgments

The work is partly supported by EPSRC under Grants GR/S524985.

## References

[1] C.W. Sohn, M.M. Chen, Microconvective thermal conductivity in disperse two phase mixture as observed in a low velocity Couette flow experiment, J. Heat Transfer, Trans. ASME 103 (1981) 47–51.
[2] A.S. Ahuja, Augmentation of heat transport in laminar flow of polystyrene suspension. I: experiments and results, J. Appl. Phys. 46 (1975) 3408–3416.
[3] A.S. Ahuja, Augmentation of heat transport in laminar flow of polystyrene suspension. II: analysis of data, J. Appl. Phys. 46 (1975) 3417–3425.
[4] G. Hetsroni, R. Rozenblit, Heat transfer to a liquid–solid mixture in a flume, Int. J. Multiphase Flow 20 (1994) 671–689.
[5] S.U.S. Choi, Enhancing thermal conductivity of fluids with nanoparticles, in: D.A. Siginer, H.P. Wang (Eds.), Developments and Applications of Non-Newtonian Flows, FED-vol. 231/MD-vol. 66, ASME, New York,, 1995 pp. 99–105.
[6] H. Masuda, A. Ebata, K. Teramae, N. Hishinuma, Alteration of thermal conductivity and viscosity of liquid by dispersing ultra-fine particles (dispersion of $\gamma$-$Al_2O_3$ $SiO_2$ and $TiO_2$ ultra-fine particles), Netsu Bussei (Japan) 4 (1993) 227–233.

[7] J.A. Eastman, S.U.S. Choi, S. Li, L.J. Thompson, S. Lee, Enhanced thermal conductivity through the development of nanofluids, in: 1996 Fall Meeting of the Materials Research Society (MRS), Boston, USA, 1996, pp. 3–11.
[8] X.W. Wang, X.F. Xu, S.U.S. Choi, Thermal conductivity of nanoparticle–fluid mixture, J. Thermophys. Heat Transfer 13 (1999) 474–480.
[9] S. Lee, S.U.S. Choi, S. Li an, J.A. Eastman, Measuring thermal conductivity of fluids containing oxide nanoparticles, J. Heat Transfer, Trans. ASME 121 (1999) 280–289.
[10] Y.M. Xuan, Q. Li, Heat transfer enhancement of nanofluids, Int. J. Heat Fluid Flow 21 (2000) 58–64.
[11] J.A. Eastman, S.U.S. Choi, S. Li, W. Yu, L.J. Thompson, Anomalously increased effective thermal conductivities of ethylene glycol-based nanofluids containing copper nanoparticles, Appl. Phys. Lett. 78 (2001) 718–720.
[12] P. Keblinski, S.R. Phillpot, S.U.S. Choi, J.A. Eastman, Mechanisms of heat flow in suspensions of nano-sized particles (nanofluids), Int. J. Heat Mass Transfer 45 (2002) 855–863.
[13] H. Xie, J. Wang, T.G. Xi, Y. Liu, F. Ai, Thermal conductivity enhancement of suspensions containing nanosized alumina particles, J. Appl. Phys. 91 (2002) 4568–4572.
[14] B.X. Wang, L.P. Zhou, X.F. Peng, A fractal model for predicting the effective thermal conductivity of liquid with suspension of nanoparticles, Int. J. Heat Mass Transfer 46 (2003) 2665–2672.
[15] S.K. Das, N. Putra, W. Roetzel, Pool boiling characteristics of nano-fluids, Int. J. Heat Mass Transfer 46 (2003) 851–862.
[16] S.K. Das, N. Putra, W. Roetzel, Pool boiling of nanofluids on horizontal narrow tubes, Int. J. Multiphase Flow 29 (2003) 1237–1247.
[17] C.H. Li, B.X. Wang, X.F. Peng, Experimental investigations on boiling of nano-particle suspensions, in: 2003 Boiling Heat Transfer Conference, Jamica, USA, 2003.
[18] C.Y. Tsai, H.T. Chien, P.P. Ding, B. Chan, T.Y. Luh, P.H. Chen, Effect of structural character of gold nanoparticles in nanofluid on heat pipe thermal performance, Mater. Lett. 58 (2003) 1461–1465.
[19] S.M. You, J.H. Kim, K.H. Kim, Effect of nanoparticles on critical heat flux of water in pool boiling heat transfer, Appl. Phys. Lett. 83 (2003) 3374–3376.
[20] P. Vassallo, R. Kumar, S. Damico, Pool boiling heat transfer experiments in silica–water nano-fluids, Int. J. Heat Mass Transfer 47 (2004) 407–411.
[21] S. Lee, S.U.S. Choi, Application of metallic nanoparticle suspensions in advanced cooling systems, in: 1996 International Mechanical Engineering Congress and Exposition, Atlanta, USA, 1996.
[22] B.C. Pak, Y.I. Cho, Hydrodynamic and heat transfer study of dispersed fluids with submicron metallic oxide particles, Exp. Heat Transfer 11 (1999) 151–170.
[23] Y.M. Xuan, W. Roetzel, Conceptions for heat transfer correlation of nanofluids, Int. J. Heat Mass Transfer 43 (2000) 3701–3707.
[24] Q. Li, Y.M. Xuan, Convective heat transfer and flow characteristics of Cu–water nanofluid, Sci. China 45E (2002) 408–416.
[25] Y.M. Xuan, Q. Li, Investigation on convective heat transfer and flow features of nanofluids, ASME J. Heat Transfer 125 (2003) 151–155.
[26] K. Khanafer, K. Vafai, M. Lightstone, Buoyancy-driven heat transfer enhancement in a two-dimensional enclosure utilizing nanofluids, Int. J. Heat Mass Transfer 46 (2003) 3639–3653.
[27] T.C. Choy, Effective Medium Theory, Oxford University Press, UK, 1999.
[28] E.J. Garboczi, J.G. Berryman, New effective medium theory for the diffusivity and conductivity of a multi-scale concrete microstructure model, Concr. Sci. Eng. 2 (2000) 88–96.
[29] R.L. Hamilton, O.K. Crosser, Thermal conductivity of heterogeneous two-component systems, I&EC Fundam. 1 (1962) 187–191.
[30] R.K. Shah, Thermal entry length solutions for the circular tube and parallel platesProceedings of 3rd National Heat and Mass Transfer Conference, vol. 1, Indian Institute of Technology, Bombay, 1975, p. HMT-11-75.
[31] G.P. Celata, M. Cumo, G. Zummo, Thermal–hydraulic characteristics of single-phase flow in capillary pipes, Exp. Thermal Fluids Sci. 28 (2004) 87–95.
[32] Z.Y. Guo, Z.X. Li, Size effect on single-phase channel flow and heat transfer at microscale, Int. J. Heat Fluid Flow 24 (2003) 284–329.
[33] R.J. Phillips, R.C. Armstrong, R.A. Brown, A.L. Graham, J.R. Abbott, A constitutive equation for concentrated suspensions that accounts for shear-induced particle migration, Phys. Fluids 4A (1992) 30–40.
[34] D.S. Wen, Y.L. Ding, Effect on heat transfer of particle migration in suspensions of nanoparticles flowing through minichannels, in: 2nd International Conference on Microchannels and Minichannels, New York, USA, 2004.